Journal of Membrane Science 618 (2021) 118629

Contents lists available at ScienceDirect

Journal of Membrane Science

journal homepage: http://www.elsevier.com/locate/memsci

# Simultaneous removal of VOCs and $PM_{2.5}$ by metal-organic framework coated electret filter media

Yu Zhang [1], Xiang He [1], Zan Zhu, Wei-Ning Wang [**], Sheng-Chieh Chen [*]

*Department of Mechanical & Nuclear Engineering, Virginia Commonwealth University, 401 West Main St., Richmond, VA, 23284, USA*

ARTICLE INFO

*Keywords:*
Indoor air quality
Metal-organic framework
$PM_{2.5}$
Volatile organic compounds
Electret filter
Holding capacity

ABSTRACT

The electret filter media coated with highly porous metal-organic frameworks (MOFs) particles, named E-MOFilter, is newly developed and evaluated for its capacity for simultaneous removal of fine particulate matters ($PM_{2.5}$) and volatile organic compounds (VOCs). Three different MOF particles, including MIL-125-$NH_2$, UiO-66-$NH_2$, and ZIF-67, were synthesized and systematically characterized. The produced MOF particles were suspended in ultrapure water and then a liquid filtration apparatus was used to deposit the MOF particles onto two electret media with different minimum efficiency reporting values (MERV 13 and 17) to form the E-MOFilters. Results showed that the MOF particles deposited in MERV 13 media more uniformly than that of MERV 17. In the PM filtration tests, results showed that the E-MOFilter gained only a few more pascals of air resistance compared with clean electret media. Besides, its PM removal efficiency was found to be close to that of clean electret media. This indicates that a uniform MOF particle deposition and negligible charge degradation from the current coating process were obtained. Further, the E-MOFilter with MIL-125-$NH_2$ particle coating not only had a decent toluene removal efficiency (>80%) but also maintained its original $PM_{2.5}$ holding capacity. This work may shed light on applying the novel E-MOFilter in the residential and commercial HVAC systems and indoor air purifiers to simultaneously and effectively remove $PM_{2.5}$ and VOCs.

## 1. Introduction

The statistical data showed that people spend about 87–90% of their time indoors [1–3]. However, indoor air quality (IAQ) has been becoming a major concern not only in developing but also developed countries. In developing counties, commercial buildings and apartments are being built and homes are being refurnished due to improved wealth. That increases the use of a large quantity of furnishings, glues, paints, etc., leading to the increase in the emission of volatile organic compounds, VOCs [4–7]. Besides, due to the high concentration of ambient fine particulate matters ($PM_{2.5}$, particulate matter with an aerodynamic diameter less than 2.5 μm), $PM_{2.5}$ can infiltrate into indoor environments [8,9]. In developed counties, indoor concentrations of some pollutants are found to be often 2–5 times higher than typical outdoor concentrations. It is mainly due to the design of lower air exchange rates for energy-efficient building construction and an increased use of synthetic building materials, furnishings, personal care products, etc. [10]. Researches have shown that VOCs and $PM_{2.5}$ can lead to acute and chronic effects on humans' respiratory and central nervous systems and eventually cause hematological problems and cancer [7,9,11,12].

To mitigate $PM_{2.5}$ for healthy indoor environments, air filters are utilized in the heating, ventilating, air conditioning (HVAC) system, and indoor air cleaners (IACs). Electret filters, with quasi-permanent electrical charges on the fibers, acquiring an additional force of electrostatic attraction, show a high initial filtration efficiency and a much lower pressure drop (ΔP) compared to mechanical filters. They have been widely used to improve the quality of indoor air in recent years [13–15]. However, to achieve a good IAQ, not only $PM_{2.5}$ but also VOCs, e.g., formaldehyde, and BTXs (benzene, toluene, xylene), should be mitigated [16–19]. Traditionally, simultaneous removal of PM and VOC pollutions is achieved by combining granular activated carbon (GAC) or other adsorbents, e.g., zeolites, with filter media, either embedded in or separately as an individual filtration module [20–22]. Both assembly strategies make the filtration module bulky and heavy. There is also an advanced high-end photocatalytic oxidation (PCO) technology applied in IACs. However, the high price and requirement of UV light source

* Corresponding author.
** Corresponding author.
*E-mail addresses:* wnwang@vcu.edu (W.-N. Wang), scchen@vcu.edu (S.-C. Chen).
[1] These authors contributed equally to the work.

https://doi.org/10.1016/j.memsci.2020.118629
Received 18 May 2020; Received in revised form 15 July 2020; Accepted 13 August 2020
Available online 27 August 2020

cause the inconvenience [23–25]. The activated carbon fiber (ACF) filters were developed to simultaneously remove PMs and VOCs [26–29]. However, the ACF is not dielectric and cannot be charged, making them less efficient for PM removal compared with electret media with the same mechanical properties (fiber diameter, porosity, and thickness).

Metal-organic frameworks (MOFs), a novel class of porous crystalline polymers, have large surface areas, tailorable pore sizes, tunable functionalities, and relatively high thermal stability and selectivity, which make them promising candidates for gas capture, gas separation and drug delivery, catalysis, sensing, etc. [30,31]. MOFs are constructed from metal ions and organic ligands. Such materials offer significant chemical and structural diversity and have outperformed the traditional porous materials (activated carbon, zeolite, alumina, and silica) in adsorption of harmful gas/vapor due to their tunable pore size and chemical functionality in a controlled manner [32–34]. Inspired by MOFs having such great potential to remove harmful gases, researchers recently coated MOFs onto mechanical filters, termed MOFilters, to remove PMs and toxic gas pollutants simultaneously [35–38]. Results demonstrated that certain inorganic toxic gas species, such as $SO_2$, $H_2S$, and $O_3$, can be removed efficiently. However, because of the use of mechanical media, the pressure drop was relatively high and PM efficiency was low [8].

In this study, for the first time electret filter media is combined with MOF particles, named E-MOFilter, to mitigate $PM_{2.5}$ and VOCs simultaneously. Three MOF particles, including MIL-125-$NH_2$, UiO-66-$NH_2$ and ZIF-67, were selected and synthesized for the fabrication of E-MOFilters. These MOFs were chosen due to their small pore sizes, high surface areas, and special functionalities, enabling a promising adsorption of VOCs [39–41]. In the aspect of electret filter, two electret filters with different minimum efficiency reporting values (MERVs), i.e., MERV 13 and MERV 17, were used as base substrates for the deposition of MOF particles. The effects of fiber diameter and porosity on the uniformity of MOF particle depositions were studied. The E-MOFilters were tested not only for their initial efficiency but also holding and adsorption capacity for $PM_{2.5}$ and toluene (a common indoor VOC pollutant). The ultimate goal of this study is to demonstrate the E-MOFilter and the developed fabrication method not only maintain the charge of electret media but also keep high removal efficiency and holding capacity for $PM_{2.5}$. Besides, the E-MOFilter has high efficiency and high adsorption capacity for VOCs.

## 2. Materials and methods

### 2.1. Electret filter media

The flat sheets of the MERV 13 and MERV 17 rated electret filter media were used for the deposition of MOF particles and subsequent PM and toluene removal tests. To be noted that the MERV 17 rated filter is equivalent to the high efficiency particulate air (HEPA) filter which has a 99.97% efficiency in the removal of 0.3 μm particles. Therefore, the MERV 17 will be labeled as 'HEPA' throughout the rest of the article. The filter specifications and scanning electron microscopy (SEM) images of these two media are summarized in Table 1. As can be seen, the HEPA media have a much smaller fiber diameter (major layer) than that of MERV 13. It is expected that the HEPA media would be relatively easier for the deposition of MOF particles onto its fibers by sieving mechanism in the liquid filtration (coating) process. Since the MERV 13 has a relatively low pressure drop and its PM removal efficiency may not be high enough, this study intended to use two layers of MERV 13, in addition to 1 layer, to see if the PM and toluene removal efficiency can be further improved. In comparison, due to the existing high pressure and good PM efficiency, the HEPA will be tested with 1 layer only.

### 2.2. Synthesis of MOFs particles

Three types of MOFs, including MIL-125-$NH_2$, UiO-66-$NH_2$ and ZIF-67, were selected and synthesized to fabricate the E-MOFilters. The chosen of them was because they not only have been applied for the VOC removal in literature due to their small pore size, high surface area, and special functionalities, but also their water stability and proper size facilitating the liquid filtration coating to the electret media, which will be shown later. The three MOFs were synthesized following the procedures reported in the literature with slight modifications [39–41]. Briefly, for MIL-125-$NH_2$, 0.797 mL titanium tetraisopropoxide (TTIP) and 0.651 g 2-aminoterephthalic acid (BDC-$NH_2$) were dissolved in the mixture of dimethylformamide (DMF)/methanol (15 mL/15 mL). Then, the mixture was transferred to a Teflon-lined steel autoclave reactor and placed in an oven at 150 °C for 15 h. The obtained yellow products were isolated by centrifugation and washed by 30 mL DMF and 30 mL methanol, respectively, for three times. Finally, the samples were dried under 50 °C overnight in vacuum. For UiO-66-$NH_2$, 1.875 g $ZrCl_4$ (pre-dissolved in a mixture of DMF/HCl, 75 mL/15 mL) and 2.011 g BDC-$NH_2$ (pre-dissolved in DMF 150 mL) were mixed and heated at 80 °C for 3 h. Then the obtained powders were isolated by centrifugation and washed with 45 mL DMF for three times. Similarly, the product was dried under vacuum at 50 °C overnight. In synthesizing ZIF-67, 0.3577 g cobalt nitrate hexahydrate (pre-dissolved in 25 mL methanol) and 0.4062 g 2-methylimidazolate (pre-dissolved in 25 mL methanol) were mixed and stirred at room temperature for 24 h. Then the obtained products were isolated by centrifugation and washed with 30 mL methanol for two times. The products were also dried under vacuum at 50 °C overnight.

### 2.3. Preparation of E-MOFilters

In general, there are many ways to incorporate MOF particles with

**Table 1**
Specification of the HEPA and MERV 13 electret media for the MOF coating [14,15].

| Types | HEPA (MERV 17) | MERV 13 |
|---|---|---|
| SEM images | 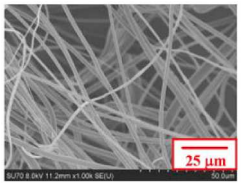  | 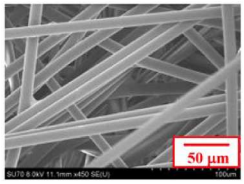  |
| Fiber diameter (μm) | 2.0 ± 0.5 (fine fibers) 80 ± 5 (coarse fibers) | 13.1 ± 0.9 |
| Thickness (mm) | 0.5 ± 0.03 (0.11 ± 0.01, excluding coarse fiber layer support) | 0.47 ± 0.02 |
| Basic weight ($g/m^2$) | 72 ± 2 (22 ± 1 without coarse fiber layer) | 75 ± 2 |
| Solidity (α) | 0.102 | 0.104 |
| Charging density ($\mu C/m^2$) | 80 | 50 |
| Initial pressure drop at 5 cm $s^{-1}$ (Pa) | 46.2 ± 0.7 | 4.5 ± 0.1 |
| Initial efficiency for 0.3 μm particles (%) | 99.97 ± 0.01 | 91.11 ± 0.23 |

the filter media, including in situ interweaving, electrospinning (physical blending of MOF nanoparticles with polymers, producing MOF-based nanofibers), freeze-drying, hot-pressing, roll-to-roll processing, air filtration deposition, etc. [36,37,42]. To choose an appropriate method for the current study, the following considerations should be taken into account in the process of combining the MOF particles with the charged fibers. Firstly, the charges of the electret media should not be degraded; secondly, the MOF particles should firmly attach to the electret media with a minimized growth of air resistance; thirdly, the transfer process is simple and cost-efficient. Reviewing the above-mentioned methods, none of them is applicable. For example, the interweaving could not tightly hold the MOF particles and particle shedding during filtration may occur; both freeze-drying and hot pressing would experience harsh temperature or pressure changes, therefore, the degradation for fiber charges is unavoidable; the roll-to-roll can also cause shedding issue; and the air filtration always leads to a non-uniform deposition of particles in depth of the media.

As none of the existing methods were appropriate, this study proposed a liquid filtration (coating) method to fabricate the E-MOFilters, which was based on the authors' previous research findings [43,44]. The choice of liquid filtration is to utilize the inherent more uniform particle deposition in liquid filtration process especially in the case of pore to particle diameter ratio is not low, e.g., 5–20. Besides, the authors have found that there was a negligible charge degradation in water soaking-drying tests for electret media [8,44]. If the MOF particles can be uniformly coated onto the fibers and in depth of the media without the formation of particle cake, the applied quantity of MOF particles and the increase of air resistance can be minimized (lower than dendrite structure in air filtration), therefore, the shielding of charge by the MOF particles should be minimized. Besides, the VOC removal efficiency should be maximized due to the high surface area of MOF particles. Fig. 1 shows the experimental setup for the MOF coating. The MOF particles were first suspended in water with a concentration of 0.02 wt %. There were still some minor loading effects causing the upper layers of the media to collect a little more MOF particles than the lower layers. Therefore, the coating flow (or filtration direction) was introduced from the back side of the filter to reduce the deposition quantity of MOF particles on the first few layers of the E-MOFilters. Thus, the attenuation of PM removal efficiency and holding capacity due to charge shielding and reduction in void space by MOF particles can be avoided [15]. The driving force for the flow circulation in the system was provided by a peristaltic pump under the flow rate of 100 mL $min^{-1}$. The coating levels and applied substrates (HEPA or MERV 13) in the fabrications of E-MOFilters are summarized in Table S1 of the Supporting Information (SI). In brief, the quantities of the coated MOFs were controlled at 5 (low), 10 (medium) and 25 (high) wt%, of the mass of MERV 13 (1 or 2 layer) and HEPA (1 layer) flat sheet with 47 mm in diameter. For example, the one with 5 wt% low coating uses MOF particles for only 3.75 g per square meter of filter.

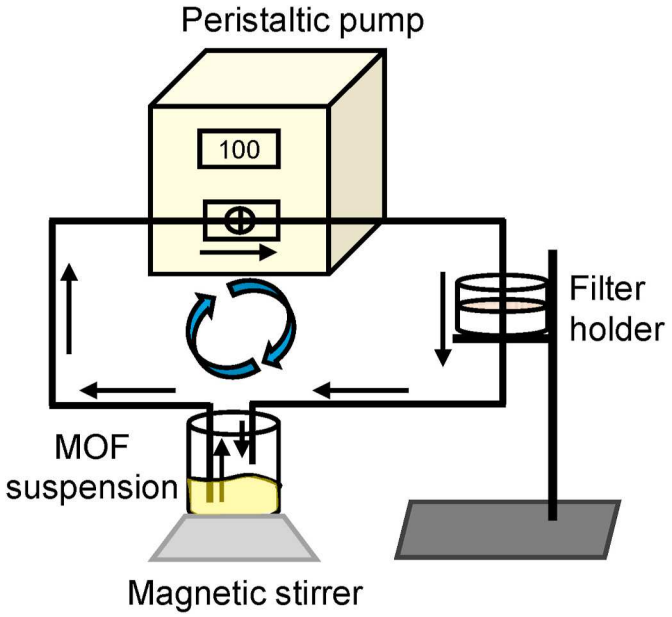


**Fig. 1.** The experimental setup to coat MOF particles onto charged filter media.

### 2.4. Characterization of MOF particles and E-MOFilters

To characterize the MOF particles, the scanning electron microscopy (SEM, HITACHI SU-70, HITACHI Corp., Tokyo, Japan), X-ray diffraction (XRD, PANalytical X'Pert Pro, Malvern PANalytical Ltd., Malvern, UK) and Fourier transform infrared spectroscopy (FT-IR, Nicolet iS50, Thermo Fisher Scientific, Waltham, MA) were utilized to probe the size, morphology, structure, and surface chemistry of the MOF particles, respectively. To measure Brunauer–Emmett–Teller (BET) surface areas of the MOF particles and E-MOFilters, $N_2$ adsorption/desorption isotherms was measured by a gas sorption analyzer (Autosorb iQ, Quantachrome Instruments Corp., Boynton Beach, FL). In addition to the surface area, the pore diameter distribution was obtained based on the density functional theory (DFT). The SEM, FT-IR and XRD analysis was also conducted for E-MOFilter to evaluate the coating uniformity of MOF particles and whether there are interactions between electret media and MOF particles.

### 2.5. Initial efficiency of E-MOFilters for PMs

After the characterization of MOF particles and E-MOFilters, E-MOFilters were evaluated for their PM and VOC removals. A difficulty was encountered when the VOC and PM removal efficiency by the E-MOFilter was intended to be measured simultaneously. It was because the filtration speed could not be remained constantly for VOC filtration as the flow needed to be switched periodically to measure the upstream or downstream particle concentration for determining the PM efficiency. Therefore, this study conducted the PM initial efficiency and PM aging tests first followed by the VOC removal efficiency and adsorption tests of the E-MOFilters and the tests with a reverse order were conducted to confirm the order would not cause many differences. Besides, a system close to the simultaneous measurement for $PM_{2.5}$ and VOC was developed, shown in Fig. S1 of SI, in which the $PM_{2.5}$ was continuously introduced to challenge the E-MOFilter (MIL-125-$NH_2$ coated MERV13 with high level) but the efficiency was not characterized. If the three results are close to each other, the experimental data obtained from the separate measurements should be applicable to the real operating condition. Table S1 summarizes the test conditions for the E-MOFilters against PM and VOC.

The initial PM removal efficiency of E-MOFilter was tested under 5 cm $s^{-1}$ face velocity (commonly used in literature) using the same experimental method of our previous study [13–15]. In brief, atomization (Model 9302, TSI Inc., Shoreview, MN) and classification (Model 3082, TSI Inc., Shoreview, MN) were utilized to produce monodisperse NaCl particles with sizes of 20–700 nm. The classified monodisperse particles were firstly neutralized to reach Boltzmann distribution to minimize and mimic the particles present in the ambient condition before being introduced to challenge the E-MOFilters. The upstream, $C_{up}$, and downstream, $C_{down}$, particle concentrations (particle $cm^{-3}$) were measured by an ultrafine condensation particle counter (UCPC, Model 3776, TSI Inc., Shoreview, MN). Then the initial size-fractioned efficiency, $\eta$ %, can be determined as:

$$\eta\,\% = \left(1 - \frac{C_{down}}{C_{up}}\right) \times 100\% \quad (1)$$

For comparison, the initial efficiency of original and discharged (by

IPA vapor) HEPA and MERV 13 electret media without coating MOF particles was also measured [45]. Because of the application of classification technique which produced monodisperse particles with low concentration, the loading effect was negligible and would not affect the PM aging tests [13–15].

### 2.6. PM aging test

The PM aging tests were conducted for the MIL-125-$NH_2$ coated E-MOFilters only as will be shown later the MIL-125-$NH_2$ performed the best VOC removal amongst the three MOFs. Similarly, E-MOFilters with three coating levels together with the original electret media will be aged under 5 cm $s^{-1}$ by PMs with a close size distribution of ambient $PM_{2.5}$ [13–15]. The average number median diameter (NMD) and mass median diameter (MMD) of the NaCl particles used to challenge the E-MOFilter media were ~80 nm and ~500 nm, respectively. The aging tests were conducted under a relative humidity (RH) of ~30%, a relatively dry condition to simulate the worst condition of aging [46]. The details of the experiments and method to determine the holding capacity, in terms of pressure drop growth versus mass load, can be found elsewhere [13–15].

### 2.7. Removal efficiency and adsorption capacity of toluene by E-MOFilters

The toluene ($C_6H_5CH_3$) as a common and representative harmful VOC in indoor air [22,47–51], was selected to challenge the E-MOFilters. The experimental setup was shown in Fig. 2 and Fig. S1 (for simultaneous $PM_{2.5}$ loading), in which a gas chromatography (GC, Agilent 7890B, Agilent Technologies Inc., Santa Clara, CA) equipped with a flame ionization detector (FID, Agilent Technologies Inc., Santa Clara, CA) was adopted to measure the toluene concentration. In the GC-FID measurement, 3 min for each run and 30 s for each sampling was set. The line of the dummy holder was used to generate the calibration curve, from 0.05 to 50 ppm, for the toluene. Results showed that the relationship between the toluene concentration and peak area had a root square of 0.999 (Fig. S2).

In this study, 5 ppm of toluene with the 5 cm $s^{-1}$ of face velocity were applied for testing. When the measurement started, the toluene flow was introduced to the dummy line first to confirm if a correct toluene concentration was used. Then the flow was switched to the E-MOFfilter line by the three-way valve. Usually, the third or fourth peak of the measurement shows the lowest peak area, i.e., the lowest toluene concentration. Thus, using Eq. (1), the initial removal efficiency of toluene, $\eta$%, can be determined from the toluene concentration measured from the dummy line representing the upstream concentration of the E-MOFilter, $C_{up}$, and the lowest concentration from the E-MOFilter line, representing the downstream concentration, $C_{down}$. When the toluene flow continued passing the E-MOFilter line, the breakthrough curve, or the adsorption capacity, was determined. To obtain the representative results, measurements for each experimental condition in toluene and PM tests were repeated four times.

## 3. Results and discussion

### 3.1. Characterization of MOF particles

Fig. 3 summarizes the characterization results of MIL-125-$NH_2$ particles, including SEM images, FT-IR spectrum, XRD patterns, and BET analysis for pore diameter, $D_{pore}$, distribution. The SEM images shown in Fig. 3 (a) reveal that the MIL-125-$NH_2$ crystals have a morphology of the tetragonal plate, which was in good agreement with that reported by Hu et al. [52]. The average length and thickness were found to be ~900 and ~300 nm, respectively, of the current MIL-125-$NH_2$ particles. The FT-IR spectrum shown in Fig. 3 (b) confirms that the produced MIL-125-$NH_2$ particles had the typical vibrational bands in the region of 1400–1700 $cm^{-1}$ representing the carboxylic acid functional group of the Ti-coordinated MOF structure. Besides, the peaks in the region of

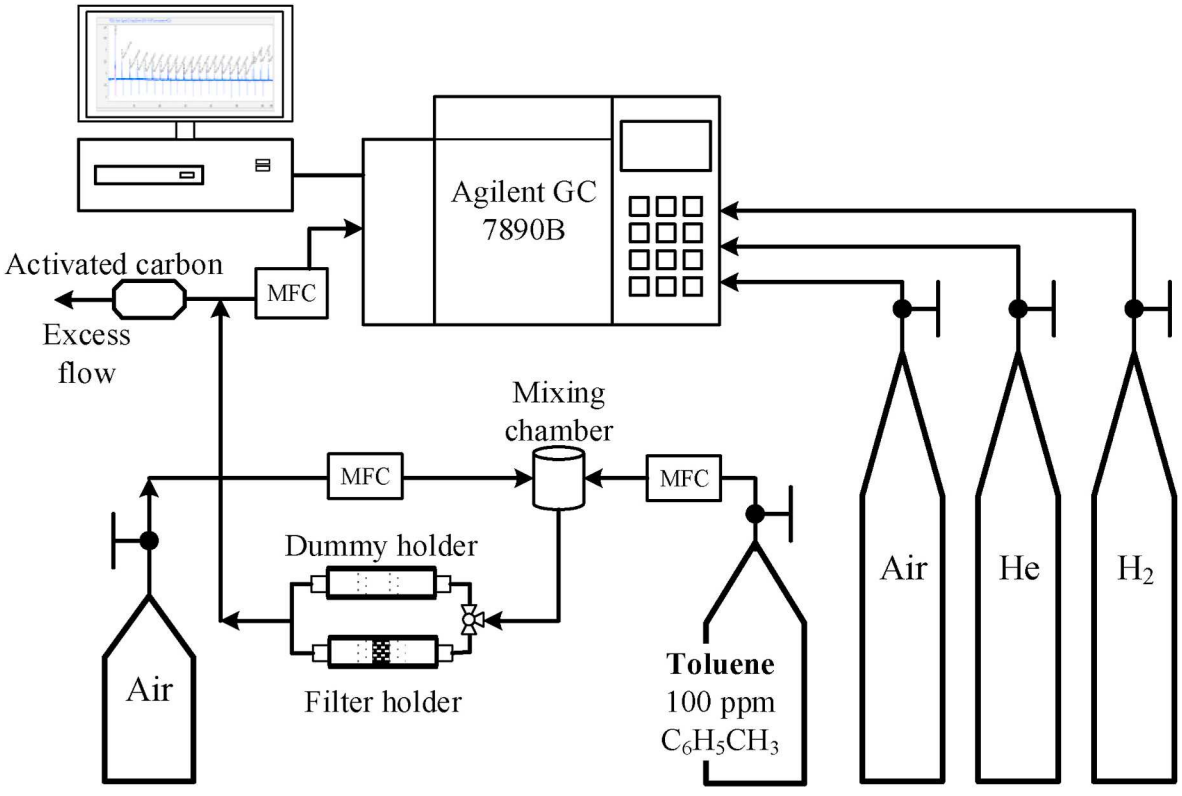


**Fig. 2.** Experimental setup for the initial removal efficiency and adsorption capacity of toluene by the E-MOFilters.

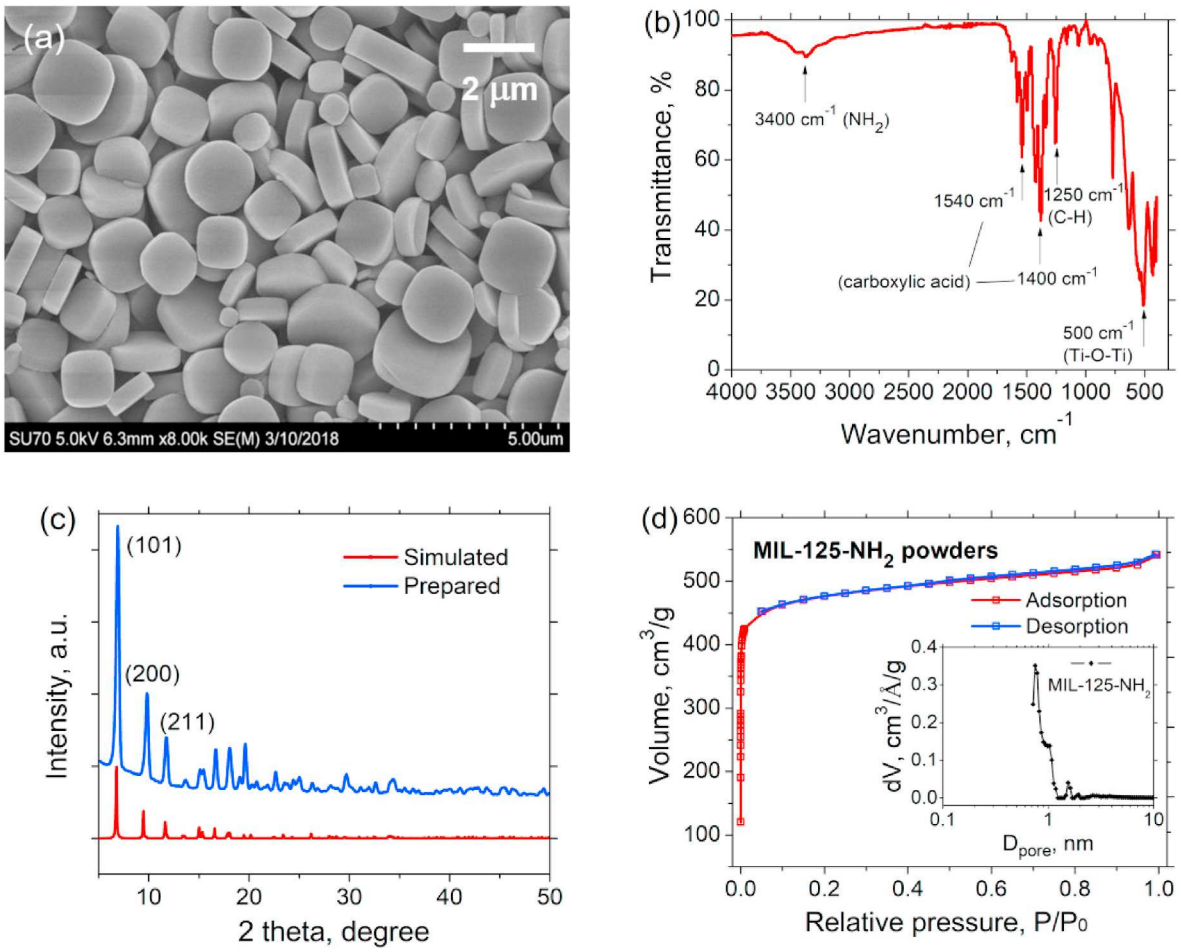


**Fig. 3.** SEM image of MIL-125-$NH_2$ (a), FT-IR spectrum of the MIL-125-$NH_2$ (b), XRD patterns of MIL-125-$NH_2$ (c), and BET analysis of MIL-125-$NH_2$ (d).

400–800 $cm^{-1}$ indicated the Ti–O–Ti vibrations, and the bands for $NH_2$ groups were present at 3500 and 3380 $cm^{-1}$. The band at 1250 $cm^{-1}$ indicated the symmetric C–H stretching vibrations in the benzene ring. All these stretch vibrations match well with that reported in the literature [52]. The XRD pattern of the synthesized MOF particles (Fig. 3 c) is in an excellent agreement with the simulated pattern, demonstrating the successful formation of the MIL-125-$NH_2$ structure. Fig. 3 (d) shows the $N_2$ adsorption/desorption isotherms of the synthesized MIL-125-$NH_2$ particles. As expected, the MOF particles exhibited type I adsorption isotherms at 77 K with no hysteresis, which verifies their microporous nature [51]. The pore diameter distribution was obtained by the DFT method and the results show that dominating pore diameter was about 0.75 nm. This value was in good agreement with that reported by Kim et al. [41], where two types of cages (octahedral with 12.5 Å and tetrahedral with 6 Å) that are accessible through microporous windows (5–7 Å) were found for the MIL-125-$NH_2$ [51]. The surface area of MIL-125-$NH_2$ was calculated to be 1871 $m^2\,g^{-1}$ using the multiple layer BET method (Table S2) which confirms the highly porous structure of the MIL-125-$NH_2$. The kinetic diameter of the toluene molecule is 5.85 Å (or 0.585 nm) [53,54], which is expected to be easily captured by the MIL-125-$NH_2$ particles due to their high surface area and suitable pore diameter.

Theoretically, there are two main mechanisms for the adsorption of toluene molecules by the MIL-125-$NH_2$ particles. Firstly, it is the pore filling mechanism due to diffusion and the forces between the adsorbents and adsorbates are Van de Waal force as a result of dipole interactions [35,47,51], which can be assigned to physisorption process. The second one is due to the hydrogen bonding between the adsorbate (toluene) and adsorbent (MIL-125-$NH_2$), which can be assigned to the chemisorption process [51,55]. According to the plausible pore filling adsorption mechanism, it is expected that the toluene molecules were easy to be trapped in the pore holes of MIL-125-$NH_2$ particles due to the matching sizes between the toluene and MIL-125-$NH_2$ particle cages. In the aspect of chemisorption, the hydrogen bonding between adsorbents and adsorbates that have ample H-donor moieties and H−acceptor moieties enhanced the capture of toluene [56,57]. To be mentioned, to include ZIF-67 and UiO-66-$NH_2$ particles allows us to understand the effects of different pore diameters and ligands of different MOFs on toluene adsorption. The characterization results of ZIF-67 and UiO-66-$NH_2$ particles for SEM, FT-IR and XRD analysis were summerized in Fig. S3. The results confirm that the ZIF-67 and UiO-66-$NH_2$ particles were also successfully synthesized.

### 3.2. *Characterization of different E-MOFilters*

Fig. 4 (a) and (b) show the pore size distribution for the HEPA and MERV 13 based E-MOFilters coated with MIL-125-$NH_2$ particles (25 wt %). The pore size distributions for the ZIF-67 and UiO-66-$NH_2$ coated HEPA E-MOFilters (25 wt%) were shown in Fig. S4. Table S2 summarizes the results of BET analysis, including surface area, pore volume, and peak pore diameter, for pure MOF particles, E-MOFilters coating with different MOF particle and two ACF filters for comparison (Fig. S4). It was found the peak pore sizes of all E-MOFilters were smaller than that of ACFs and the total surface areas of E-MOFilters were close to that of ACFs. It is expected the toluene removal efficiency between E-MOFilters and ACFs are comparable. The detailed discussion will be presented in the following. Compared with the MIL-125-$NH_2$ particles (Fig. 3 d), the MIL-125-$NH_2$ coated E-MOFilters remained a similar peak pore diameter

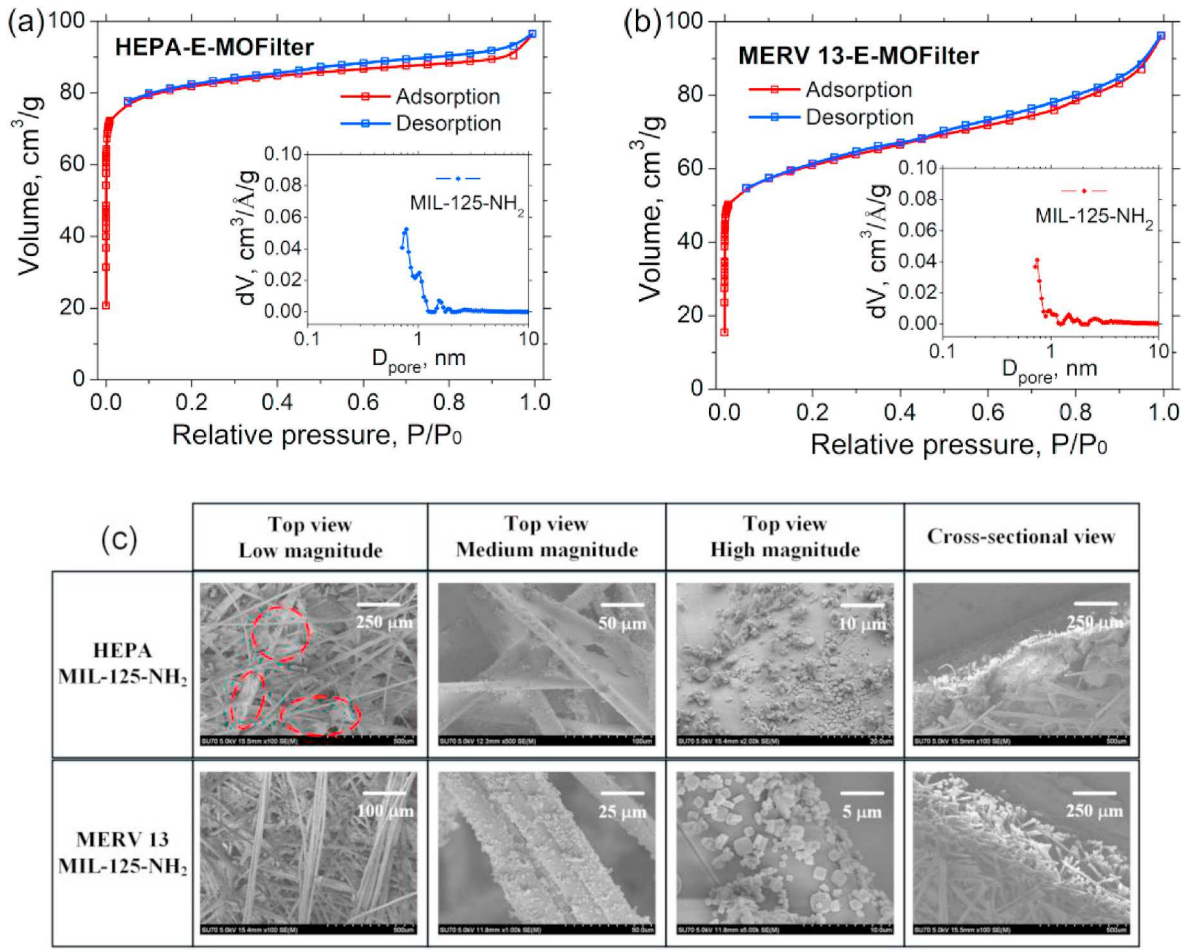


**Fig. 4.** BET analysis for MIL-125-$NH_2$ coated HEPA E-MOFilter (a) and MERV 13 E-MOFilter (b), and SEM images of MIL-125-$NH_2$ depositions on two E-MOFilters (c).

of ~0.8 nm (Table S1). That is, the coated MIL-125-$NH_2$ particles contributed most of the microporous structures of the E-MOFilter, and a certain level of removal efficiency for toluene is expected. However, the pore volume for the pure MIL-125-$NH_2$ particles is much higher than that of E-MOFilters.

To examine if there are interactions between MOFs and electret media during coating, the FTIR and XRD characterization of the bare MERV 13 electret filter, MIL-125-$NH_2$ particles and MIL-125-$NH_2$ coated E-MOFilters was conducted. The comparison of the FTIR spectra and XRD patterns amongst MERV 13, MIL-125-$NH_2$ particles and E-MOFilter is shown in Fig. S5 of SI. As can be seen, the E-MOFilter remains both functional groups and crystal structures of MERV 13 media (polypropylene) and the MIL-125-$NH_2$ particles, a superposition from the two materials. It is concluded that the coating of MOFs onto the electret media by liquid filtration method was a physical phenomenon, i.e. no interaction caused between MOFs and electret media.

Under the high coating level of 25 wt%, Fig. 4 (c) shows the SEM images of the depositions for MIL-125-$NH_2$ particles in HEPA (first row) and MERV 13 (second row) based E-MOFilters. The cross-sectional views of the two E-MOFilters are shown in the last column of Fig. 4 (c). It is seen that the MOF particles were more uniformly deposited in MERV 13 based E-MOFilter, not only on individual fibers but also in depth (the cross-sectional view), than that of HEPA filter. In different magnitudes, from an overall view to the view with zoomed in of the filter media, it was found the smaller pore sizes and higher packing density (fine fiber part) of HEPA filters caused the occurrence of bridging and clogging in many portions of the filter, highlighted with circles, especially at interstitial spaces between fibers. Similar results were found for the low- and medium-level coated HEPA based E-MOFilter as the media pore to MOF particle size ratio dominated the coating uniformity. In the coating of ZIF-67 particles, as its average size is close to that of MIL-125-$NH_2$ particles (Fig. S3), a non-uniformity of coating is expected. However, the effects were minor when coating UiO-66-$NH_2$ particles to the HEPA media, which was due to their small sizes (~250 nm, Fig. S3). Because of the small size of UiO-66-$NH_2$, this study found that they were not easy to be coated onto MERV 13 and a longer coating time is needed.

As will be shown later, the E-MOFilter coated with MIL-125-$NH_2$ particles had a better toluene removal efficiency than that of UiO-66-$NH_2$ and ZIF-67 particles, therefore, the results of MIL-125-$NH_2$ E-MOFilters will be focused and discussed in the following. To be concluded that from the coating experiments, without considering the adsorption ability amongst different MOFs, the ratio of the media pore size to MOF particle diameter is a crucial parameter determining if a uniform deposition can be achieved.

### 3.3. Initial efficiency of E-MOFilters (MIL-125-$NH_2$) for PMs

In order to investigate the effects of MOF coating on the performance of E-MOFilter against PMs, the size-fractioned efficiency of E-MOFilters was measured. Fig. 5 shows the results for the MIL-125-$NH_2$ coated MERV 13 (2 layers) E-MOFilters with different coating levels measured at 5 cm $s^{-1}$ face velocity. The original MERV 13 without MIL-125-$NH_2$ particles and the discharged MERV 13 by isopropyl alcohol (IPA) vapor were also tested to determine the efficiency decline due to charge degradation and remainder from the coating. The decline of PM removal efficiency gets severer with increasing loading level due to charge

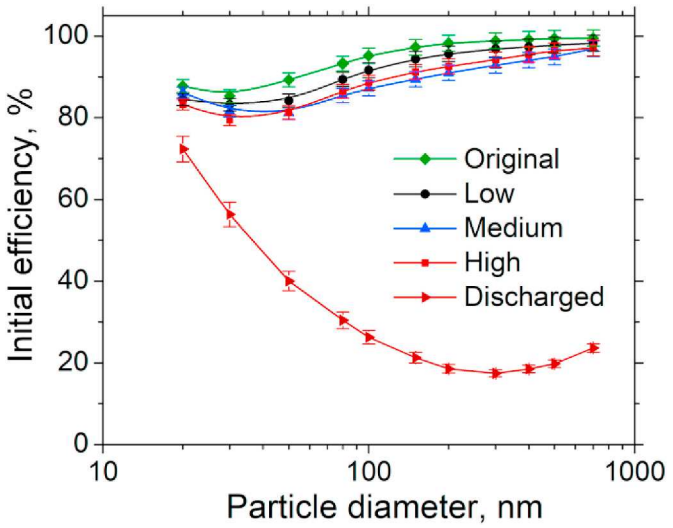


**Fig. 5.** Initial size-fractioned efficiency of MERV 13 E-MOFilter coated with different levels of MIL-125-$NH_2$ particles.

shielding, nevertheless, the declines in all particle sizes were less than 10% for all three levels of coating. The E-MOFilter with a high-level MOF coating had a higher efficiency in the removal of larger particles than that with medium-level MOF coating, which should be attributed to loading effects. There were substantial efficiency differences between the E-MOFilters with that of discharged one, indicating a negligible efficiency degradation due to the coating. Although more MIL-125-$NH_2$ coating should enhance the capture of toluene, to compromise the decay of PM efficiency and the increase of pressure drop, and the decline of PM holding capacity (shown later), low or medium level of coating might be more desirable. A similar result with only minor efficiency decline was obtained for the HEPA E-MOFilters coated with high level of MIL-125-$NH_2$ (Fig. S6).

One question that may be asked is if the shedding of MOF particles can occur during the filtration of E-MOFilters. To address this issue, the MERV 13 E-MOFilters coated with all three levels of MIL-125-$NH_2$ were tested. In the experiments, E-MOFilters were blown with clean air at face velocities of 5 and 10 cm $s^{-1}$, the common filtration velocities, and a raised velocity of 30 cm $s^{-1}$ for challenging the stability of the current coating method. The air downstream of the filter was introduced to the UCPC which was operated with the accumulation counting mode. Ten times with 1 min for each was run. Table S3 shows the results of the particle shedding, in which the average values and standard deviations were rounded to the nearest integer. It is seen the shedding of particles does increase with increasing velocity and coating level. However, a quick calculation shows that there will be only ~0.001–0.01% of MOF particles released for the high coating E-MOFilter being operated at 30 cm $s^{-1}$ for 7/24 for a year. Therefore, the coating method presented here maintains the merits of electret media, including high efficiency and low pressure drop, and has a negligible shedding effect.

### 3.4. Performance of E-MOFilters on PM loading

For an IAC or HVAC filter, in addition to the initial efficiency, its performance over a period of operation, e.g., a few months, is of great concern. A commonly applied criterion is the PM holding capacity, i.e., the loaded PM mass versus the pressure drop growth which relates to the energy consumption in operating the filtration. Besides, as an electret media, its efficiency usually declines from the beginning of the operation, due to charge shielding, until loading effects occur and beat the decline. Therefore, this time-dependent and dynamic filter efficiency should also be considered as the second criterion. Since the focus of this study was to examine if the coating of MOF particles could deteriorate the performance of the electret media, only the two criteria about PM loading will be compared, as follows. The insights into PM loading characteristics for electret media, i.e., mechanisms of charge decay, transitions in the pressure drop growth curve, loading effects on efficiency enhancement, etc., can be found elsewhere [46], thus, will not be discussed here.

Fig. 6 compares the $PM_{2.5}$ holding capacities of the clean MERV 13 and MERV 13 E-MOFilters coated with different levels of MIL-125-$NH_2$ particles. The initial pressure drop of these filters are also shown in the figure and it was found the increase of initial pressure drops were very minor with only 1.5 and 3.7 Pa for the low and medium coated E-MOFilters, respectively. In comparison, the highly coated E-MOFilter gained a significant pressure drop (12.5 Pa). In the $PM_{2.5}$ aging tests, the endpoint was set at 1.0 in-$H_2O$ (249 Pa) and the more mass of PMs can be collected the better the filter is. As expected, the clean MERV 13 had the highest holding capacity (19.1 g $m^{-2}$) and it was about 10, 25, and 50% higher than that of the low, medium, and high coating, respectively. It becomes clear that, in terms of deterioration of PM holding capacity, the E-MOFilters with low and medium coating should be acceptable, whereas, not for the high coating.

Fig. 7 compares dynamic size-fractioned efficiency at different mass loads amongst original MERV 13 and E-MOFilters with the three coating levels (MIL-125-$NH_2$). The curves in each figure correspond to the efficiencies at initial (0 loading), minimum values (onset of efficiency increase for most particle sizes), pressure drop at 0.5 in-$H_2O$, and 1.0 in-$H_2O$ (endpoint of aging), respectively. The minimum efficiency is important as it represents the worst filtration condition in the use of electret-based filters [46]. When the loading started, due to charge degradation the size-fractioned efficiency of these electret filters began declining (except for small particles in original and low coating level media) from their initial efficiency to the minimum efficiency, after which filter efficiency kept increasing because of loading effects [8,46].

The minimum efficiencies of low and medium coated E-MOFilters remain to be greater than 80%, whereas the minimum efficiency for the one with high MOF coating was found to be less than 80%. To be highlighted, the small particles (<50 nm) did not or almost had no efficiency reduction during the PM loading. This was because their deposition mechanism inherently relied mainly on diffusion rather than electrostatic force. From Fig. 7, it is seen the dynamic efficiency curves of E-MOFilters did differ quite much from the original MERV 13, nevertheless, the trend remained a very close characteristic as the original MERV 13. In summary, the test results for PM loading for E-

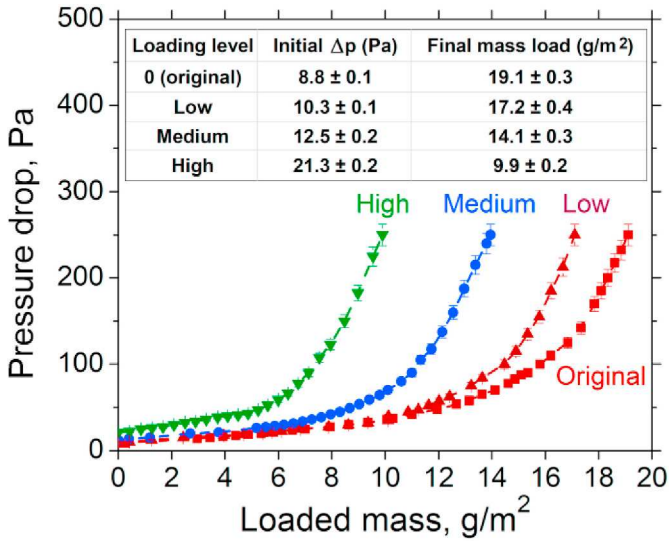


**Fig. 6.** Effects of the MOF loading on the evolution of pressure drop of the MERV 13 E-MOFilters during filtration.

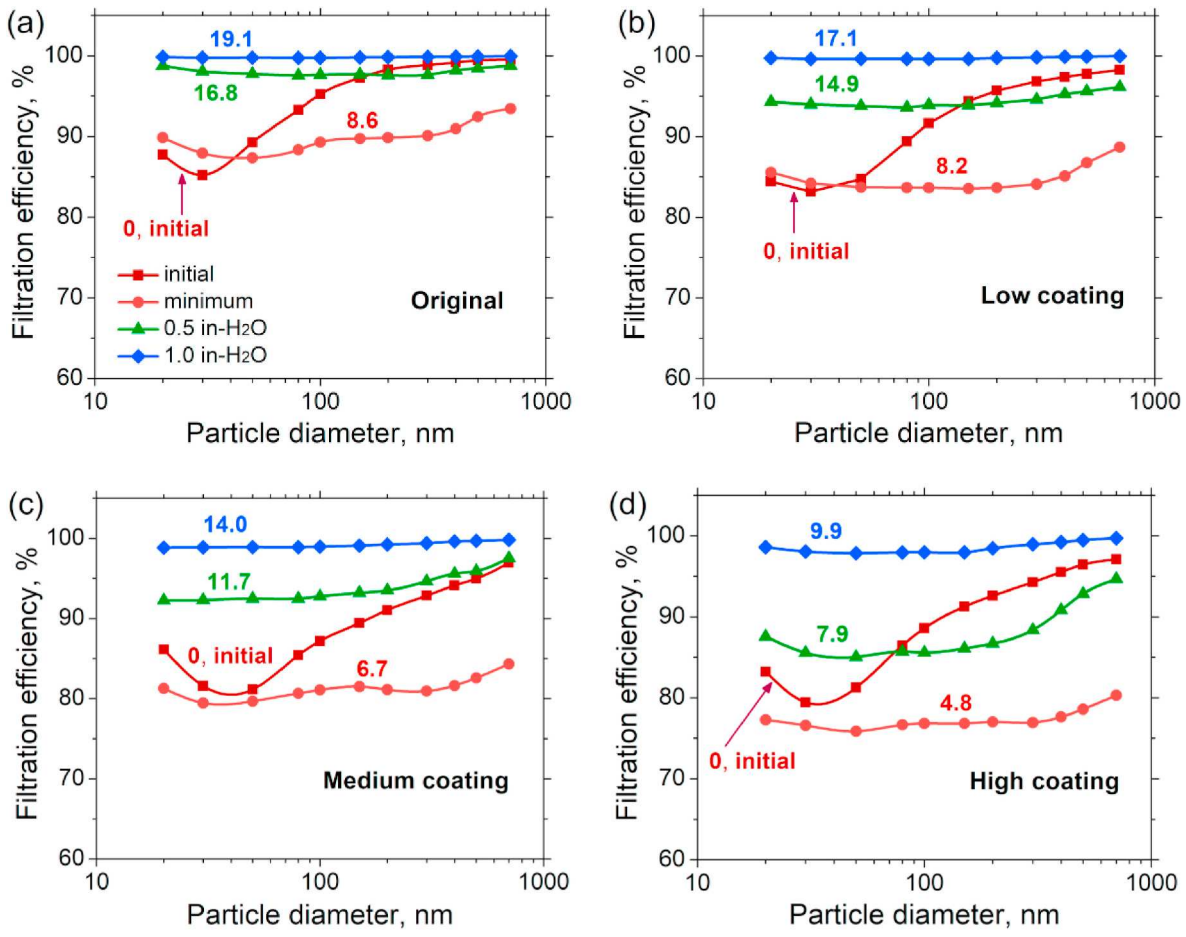


**Fig. 7.** Dynamic size-fractioned efficiency of original (a), low coating (b), medium coating (c), and high coating (d) MERV 13 filters along PM aging process.

MOFilters confirmed the current coating method, liquid filtration and from back to front, did not degrade the fiber charge too much or alter the fiber structure of electret media.

### 3.5. Performance of E-MOFilters for toluene removal

#### 3.5.1. Initial removal efficiency

In the previous section, the performances of E-MOFilters for PM removal have been demonstrated to be comparable to that of the original electret filters, especially for the E-MOFilters with low and medium

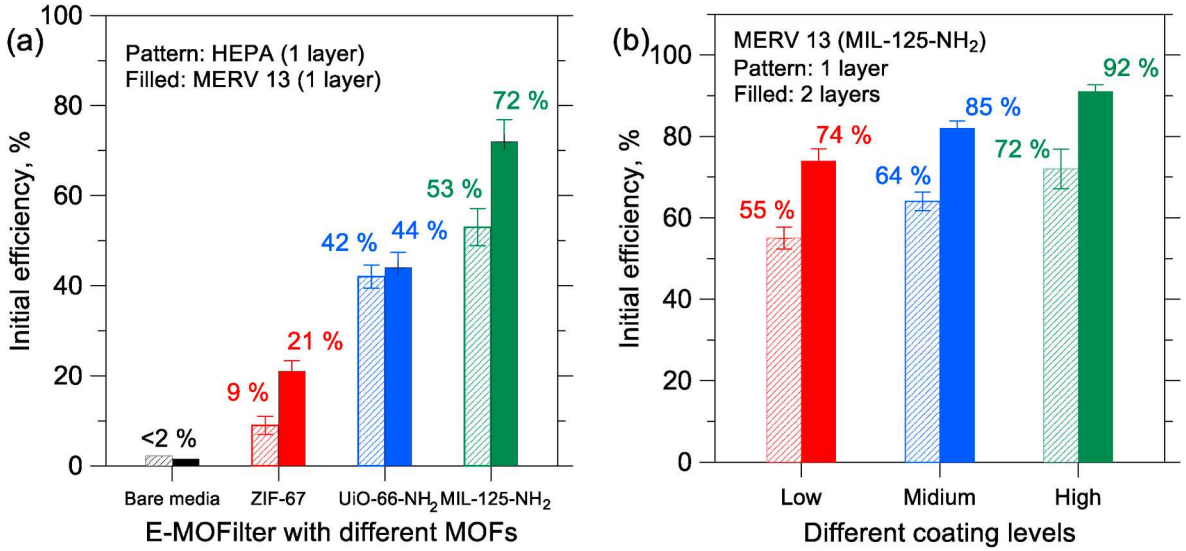


**Fig. 8.** (a) Comparison of initial toluene removal efficiency between HEPA and MERV 13 based E-MOFilters coated with different MOF particles (25 wt% high level). (b) Comparison of initial toluene removal efficiency by 1 and 2 layers of MERV 13 filter coated with different levels of MIL-125-$NH_2$ particles.

level coating. In this section, the removal of toluene by the E-MOFilers will be quantitatively compared amongst different base substrates, MERV 13 (1 or 2 layers) and HEPA, and different MOF particles with different levels of coating.

Fig. 8 (a) compares the initial toluene removal efficiency under 5 cm $s^{-1}$ face velocity between the MERV 13 (1 layer) and HEPA (1 layer) E-MOFilters coated with high levels (25 wt%) of the three MOF particles. The removal efficiency by the bare electret filter is also included, and it was found to be less than 2% for both HEPA and MERV 13 media, indicating the toluene removal was mainly attributed to the MOF particles. An order of MIL-125-$NH_2$ > UiO-66-$NH_2$ > ZIF-67 for the toluene removal efficiency was found for both MERV 13 and HEPA E-MOFilters. In comparison, the MERV 13 exhibited better performance than HEPA towards the toluene removal when coated with MOF particles. This was attributed to the uniformity of coating influenced by the ratio of media pore to MOF particle diameter as discussed in section 3.2. The ZIF-67 (29% with MERV 13) and UiO-66-$NH_2$ (44% with MERV 13) may not be qualified to be applied in the E-MOFilter as their efficiencies were too low. While for MIL-125-$NH_2$, the efficiency was as good as 72%. This promising result should be highlighted because the method proposed within this study does prove not only the coating method retains the charge of electret media but also the coated MOF particles can remove toluene efficiently. From the above discussion, the HEPA, ZIF-67, and UiO-66-$NH_2$ could be excluded from the further tests in examining the effects of the coating level and using two layers of MERV 13 on toluene removal efficiency and adsorption capacity.

Fig. 8 (b) compares the toluene removal efficiency amongst 1 and 2 layers of MERV 13 E-MOFilters coated with three levels of MIL-125-$NH_2$ under 5 cm $s^{-1}$ face velocity. Reasonably, the efficiency increases with one additional layer of MERV 13 and coating level of MOF particles, however, not as large as expected. An average improvement of ~20% from 1 layer to 2 layers and ~8% from increasing coating level was obtained. To be mentioned, the 2-layer low coated E-MOFilter already had a decent efficiency of 74%. Besides, 2 layers of MERV 13 is required as it would enhance the PM removal efficiency and toluene adsorption capacity which will be shown later.

From the results of the initial toluene removal efficiency shown in Fig. 8, it becomes clear that the ratio of the filter pore size to MOF particle size is a crucial parameter for achieving a good coating and thus a good toluene removal. Besides, the amino functional group in ligand should also contribute to the toluene removal via chemisorption. Although HEPA filter has high initial efficiency, however, as has been reported in literature [8,46], electret HEPA filter has a much lower holding capacity for PM, therefore, applying MERV 13 (two layers here) as the coating substrate is more desirable. Its larger pore size increases the flexibility to be the base substrate for coating many other MOF particles with different sizes, which may extend the applications for removing other gaseous pollutants.

### 3.5.2. Toluene adsorption capacity

Fig. 9 shows the toluene adsorption capacity, or breakthrough curves, of the 2-layer MERV 13 E-MOFilter coated with different levels of MIL-125-$NH_2$. The breakthrough curves for 2 ACF filters used in respirators for welding workers and the 1-layer E-MOFilter with high coating are also shown for comparison. It can be seen that the adsorption capacity increases substantially with increasing coating quantity. The two ACFs do have higher initial efficiency, ~90–95%, however, their adsorption capacity is only comparable with the low coating E-MOFilter, and worse than the medium and high coating E-MOFilters. The capacity of the 1-layer highly coated E-MOFileter is close to that of medium coated 2-layer E-MOFilter but lower than the 2-layer highly coated one, indicating the doubling of MOF particles does increase the toluene adsorption capacity. A rough calculation considering the area of the right triangle upper the breakthrough curve shows the captured quantity of toluene is about double by the 2-layer E-MOFilter.

Fig. 9 also compares the adsorption capacity amongst the E-MOFilters evaluated for PM loading first (particle first), toluene adsorption first (toluene first), and simultaneously but without characterizing PM efficiency and loading (simultaneous) to understand whether the treatment order and separate measurement would lead to different results. Results showed that the adsorption capacity for treating toluene first was only slightly better than that of particle first and the simultaneous one, the current results of E-MOFiltters for different coating levels and different MOFs are applicable for the real operation when particle and toluene filtrations are taking place simultaneously. Based on the decent results obtained, the newly developed method for the fabrication of E-MOFilter should be extended to the applications in making filter media for IAC, HVAC, and respirator filters. Although the 2-layer highly coated E-MOFilter had an outstanding performance towards the removal of toluene, an overall evaluation on the trade-off of gained pressure drop

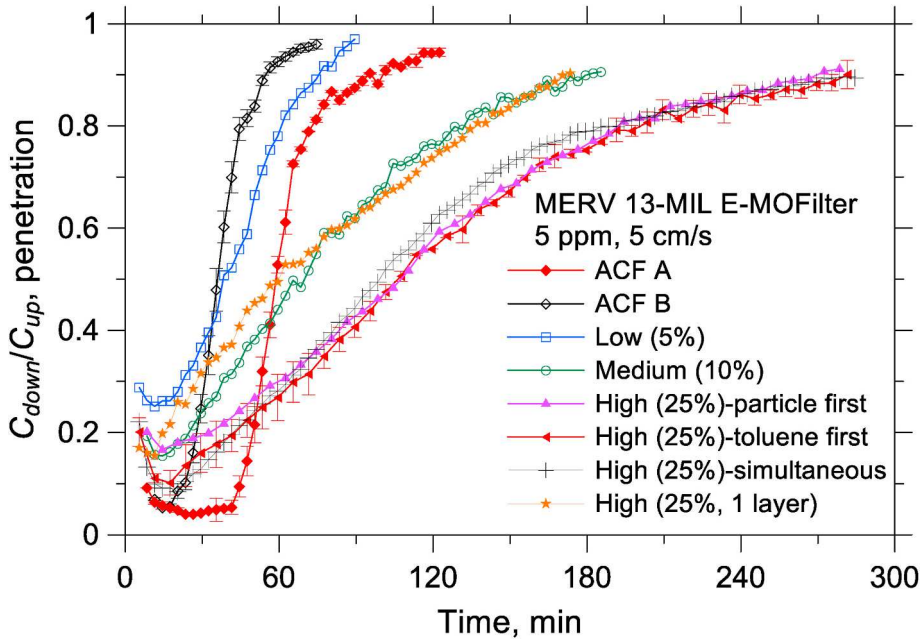


**Fig. 9.** Comparison of breakthrough curves amongst ACFs and MERV 13 based E-MOFilters coated with different levels of MIL-125-$NH_2$ particles.

and charge degradation causing the decline of PM initial efficiency and PM holding capacity is needed. Both low and medium coated 2-layer MOFilter would be good choices for now before an optimized coating condition and better MOF particles are found.

## 4. Conclusion

Three MOF particles, including MIL-125-$NH_2$, UiO-66-$NH_2$ and ZIF-67, were synthesized, characterized, and coated to a MERV 13 and a HEPA grade electret filter media to form E-MOFilters for the simultaneous removal of fine particulate matters ($PM_{2.5}$) and volatile organic compounds (VOCs). As for the MOF coating, 5, 10 and 25 wt% of the mass of the MERV 13 and HEPA media were applied to figure out which level is the most appropriate, in terms of low increase of air resistance, low charge degradation, and sufficient VOC removal efficiency and adsorption capacity. A series of measurements were conducted to test the initial efficiency and holding/adsorption capacity of PM and toluene by the E-MOFilters.

The characterization results show that the MOF particles were successfully synthesized with similar morphology, size, surface area, pore diameter, FT-IR spectrum, and XRD patterns to those reported in the literature. The PM removal performances, in terms of initial efficiency, holding capacity, and dynamic efficiency, of the low and medium coated E-MOFilter were found to be comparable to the original MERV 13. However, the highly coated one gained an essential air resistance and had a much lower PM holding capacity. The comparison of the time-dependent size-fractioned efficiency along the aging between E-MOFilter and original electret media shows that they have a similar trend of efficiency decline due to charge shielding and efficiency enhancement caused by loading effects. This indicates the coating method presented here does not significantly deteriorate the charge density and change the fibrous structure to a considerable extent.

The initial toluene removal efficiency of the MERV 13 E-MOFilters coated with MIL-125-$NH_2$ reaches 74% and 85% for the low and medium coating levels, respectively. It was found the pore of filter media to MOF particle size is a crucial parameter for achieving a good coating and good toluene removal. Although HEPA filter had high initial efficiency, its lower holding capacity for PM and small pore size result in clogging during the MOF coating. Therefore, using MERV 13 as the coating substrate is more desirable. From the toluene adsorption capacity results, it is seen the newly developed MERV 13 E-MOFilter had a comparable capacity to that of two ACF media used in the respirators for welding workers. The low medium and high coating MOFilter predominated the ACFs. However, to consider the deterioration of the PM removal for the highly coated E-MOFilter, the parameters of the low and medium coated E-MOFilter may be more desirable to be applied in the designs of IAC, HVAC, and respirator filters.

## Author statement

Yu Zhang: Data curation, original draft

Xiang He: Data curation, Methodology, Writing - review & editing

Zan Zhu: Formal analysis, Visualization

Wei-Ning Wang: Conceptualization, Supervision, Writing - review & editing

Sheng-Chieh Chen: Conceptualization, Funding acquisition, Project administration, Writing - review & editing

## Declaration of competing interest

The authors declare that they have no known competing financial interests or personal relationships that could have appeared to influence the work reported in this paper.

## Acknowledgement

This work was supported by the members of the Center for Filtration Research: A.O. Smith Company, Applied Materials Inc., BASF Corporation, Boeing Company, Corning Inc., China Yancheng Environmental Protection Science and Technology City, Cummins Filtration Inc., Donaldson Company, Inc., Ford Motor Company, Guangxi Wat Yuan Filtration System Co., Ltd, Mott Corporation, MSP Corporation; Samsung Electronics Co., Ltd., Parker-Hannifin Corporation, Shigematsu Works Co. Ltd.; TSI Inc.; W. L. Gore & Associates, Inc., Xinxiang Shengda Filtration Technique Co. Ltd., and the affiliate member National Institute for Occupational Safety and Health (NIOSH). W.N.W. acknowledges the financial support from National Science Foundation (CMMI-1727553) for MOFs manufacturing.

## Appendix A. Supplementary data

Supplementary data to this article can be found online at https://doi.org/10.1016/j.memsci.2020.118629.

## References

[1] N.E. Klepeis, W.C. Nelson, W.R. Ott, J.P. Robinson, A.M. Tsang, P. Switzer, J. V. Behar, S.C. Hern, W.H. Engelmann, E. Epidemiology, The National Human Activity Pattern Survey (NHAPS): a resource for assessing exposure to environmental pollutants, J. Expo. Sci. Environ. Epidemiol. 11 (2001) 231–252.

[2] S. Brasche, W. Bischof, Daily time spent indoors in German homes–baseline data for the assessment of indoor exposure of German occupants, Int. J. Hyg Environ. Health 208 (2005) 247–253.

[3] C. Schweizer, R.D. Edwards, L. Bayer-Oglesby, W.J. Gauderman, V. Ilacqua, M. J. Jantunen, H.K. Lai, M. Nieuwenhuijsen, N. Kunzli, Indoor time-microenvironment-activity patterns in seven regions of Europe, J. Expo. Sci. Environ. Epidemiol. 17 (2007) 170–181.

[4] C. Jiang, S. Li, P. Zhang, J. Wang, Pollution level and seasonal variations of carbonyl compounds, aromatic hydrocarbons and TVOC in a furniture mall in Beijing, China, Build. Environ. 69 (2013) 227–232.

[5] K. Huang, J. Song, G. Feng, Q. Chang, B. Jiang, J. Wang, W. Sun, H. Li, J. Wang, X. Fang, Indoor air quality analysis of residential buildings in northeast China based on field measurements and longtime monitoring, Build. Environ. 144 (2018) 171–183.

[6] T. Chang, D. Ren, Z. Shen, Y. Huang, J. Sun, J. Cao, J. Zhou, H. Liu, H. Xu, C. Zheng, H. Pan, C. He, Indoor air pollution levels in decorated residences and public places over xi'an, China, Aerosol Air Qual. Res. 17 (2017) 2197–2205.

[7] Q. Chen, H. Sun, J. Zhang, Y. Xu, Z. Ding, The hematologic effects of BTEX exposure among elderly residents in Nanjing: a cross-sectional study, Environ. Sci. Pollut. Res. 26 (2019) 10552–10561.

[8] S. Li, D.R. Chen, F. Zhou, S.C. Chen, Effects of relative humidity and particle hygroscopicity on the initial efficiency and aging characteristics of electret HVAC filter media, Build. Environ. 171 (2020), 106669.

[9] D.Y.H. Pui, S.C. Chen, Z. Zuo, PM 2.5 in China: measurements, sources, visibility and health effects, and mitigation, Particuology 13 (2014) 1–26.

[10] EPA. https://www.epa.gov/report-environment/indoor-air-quality, 2017.

[11] D.A. Sarigiannis, S.P. Karakitsios, A. Gotti, I.L. Liakos, A. Katsoyiannis, Exposure to major volatile organic compounds and carbonyls in European indoor environments and associated health risk, Environ. Int. 37 (2011) 743–765.

[12] Y. Du, X. Xu, M. Chu, Y. Guo, J. Wang, Air particulate matter and cardiovascular disease: the epidemiological, biomedical and clinical evidence, J. Thorac. Dis. 8 (2016) E8–E19.

[13] M. Tang, D. Thompson, D.Q. Chang, S.C. Chen, D.Y.H. Pui, Filtration efficiency and loading characteristics of PM2.5 through commercial electret filter media, Separ. Purif. Technol. 195 (2018) 101–109.

[14] M. Tang, S.C. Chen, D.Q. Chang, X. Xie, J. Sun, D.Y.H. Pui, Filtration efficiency and loading characteristics of PM2.5 through composite filter media consisting of commercial HVAC electret media and nanofiber layer, Separ. Purif. Technol. 198 (2018) 137–145.

[15] D.Q. Chang, C.Y. Tien, C.Y. Peng, M. Tang, S.C. Chen, Development of composite filters with high efficiency, low pressure drop, and high holding capacity PM2.5 filtration, Separ. Purif. Technol. 212 (2019) 699–708.

[16] Z. Du, J. Mo, Y. Zhang, Q. Xu, Benzene, toluene and xylenes in newly renovated homes and associated health risk in Guangzhou, China, Build. Environ. 72 (2014) 75–81.

[17] T. Ohura, T. Amagai, X. Shen, S. Li, P. Zhang, L. Zhu, Comparative study on indoor air quality in Japan and China: characteristics of residential indoor and outdoor VOCs, Atmos. Environ. 43 (2009) 6352–6359.

[18] C. Walgraeve, K. Demeestere, J. Dewulf, K. Van Huffel, H. Van Langenhove, Diffusive sampling of 25 volatile organic compounds in indoor air: uptake rate determination and application in Flemish homes for the elderly, Atmos. Environ. 45 (2011) 5828–5836.

[19] B.F. Yu, Z.B. Hu, M. Liu, H.L. Yang, Q.X. Kong, Y.H. Liu, Review of research on air-conditioning systems and indoor air quality control for human health, Int. J. Refrig. 32 (2009) 3–20.
[20] X. Zhao, Q. Ma, G. Lu, VOC removal: comparison of MCM-41 with hydrophobic zeolites and activated carbon, Energy Fuels 12 (1998) 1051–1054.
[21] W.K. Jo, C.H. Yang, Granular-activated carbon adsorption followed by annular-type photocatalytic system for control of indoor aromatic compounds, Separ. Purif. Technol. 66 (2009) 438–442.
[22] F. Rezaei, G. Moussavi, A.R. Bakhtiari, Y. Yamini, Toluene removal from waste air stream by the catalytic ozonation process with MgO/GAC composite as catalyst, J. Hazard Mater. 306 (2016) 348–358.
[23] J. Zhao, X. Yang, Photocatalytic oxidation for indoor air purification: a literature review, Build. Environ. 38 (2003) 645–654.
[24] A. Vohra, D.Y. Goswami, D.A. Deshpande, S.S. Block, Enhanced photocatalytic disinfection of indoor air, Appl. Catal., B 64 (2006) 57–65.
[25] L. Zhong, F. Haghighat, Photocatalytic air cleaners and materials technologies – abilities and limitations, Build. Environ. 91 (2015) 191–203.
[26] D. Das, V. Gaur, N. Verma, Removal of volatile organic compound by activated carbon fiber, Carbon 42 (2004) 2949–2962.
[27] S. Yang, Z. Zhu, F. Wei, X. Yang, Carbon nanotubes/activated carbon fiber based air filter media for simultaneous removal of particulate matter and ozone, Build. Environ. 125 (2017) 60–66.
[28] X. Zhang, B. Gao, A.E. Creamer, C. Cao, Y. Li, Adsorption of VOCs onto engineered carbon materials: a review, J. Hazard Mater. 338 (2017) 102–123.
[29] L. Zhu, D. Shen, K.H. Luo, A critical review on VOCs adsorption by different porous materials: species, mechanisms and modification methods, J. Hazard Mater. 389 (2020), 122102.
[30] H. Furukawa, K.E. Cordova, M. O'Keeffe, O.M. Yaghi, The chemistry and applications of metal-organic frameworks, Science 341 (2013) 1230444.
[31] J.B. DeCoste, G.W. Peterson, Metal-organic frameworks for air purification of toxic chemicals, Chem. Rev. 114 (2014) 5695–5727.
[32] A. Schneemann, V. Bon, I. Schwedler, I. Senkovska, S. Kaskel, R.A. Fischer, Flexible metal-organic frameworks, Chem. Soc. Rev. 43 (2014) 6062–6096.
[33] W. Lu, Z. Wei, Z.Y. Gu, T.F. Liu, J. Park, J. Park, J. Tian, M. Zhang, Q. Zhang, Gentle III, Tuning the structure and function of metal–organic frameworks via linker design, Chem. Soc. Rev. 43 (2014) 5561–5593.
[34] K.K. Tanabe, S.M. Cohen, Postsynthetic modification of metal-organic frameworks–a progress report, Chem. Soc. Rev. 40 (2011) 498–519.
[35] Y. Zhang, S. Yuan, X. Feng, H. Li, J. Zhou, B. Wang, Preparation of nanofibrous metal-organic framework filters for efficient air pollution control, J. Am. Chem. Soc. 138 (2016) 5785–5788.
[36] X. Ma, Y. Chai, P. Li, B. Wang, Metal-organic framework films and their potential applications in environmental pollution control, Acc. Chem. Res. 52 (2019) 1461–1470.
[37] Y. Chen, S. Zhang, S. Cao, S. Li, F. Chen, S. Yuan, C. Xu, J. Zhou, X. Feng, X. Ma, B. Wang, Roll-to-Roll production of metal-organic framework coatings for particulate matter removal, Adv. Mater. 29 (2017).
[38] S. Ma, M. Zhang, J. Nie, B. Yang, S. Song, P. Lu, Multifunctional cellulose-based air filters with high loadings of metal–organic frameworks prepared by in situ growth method for gas adsorption and antibacterial applications, Cellulose 25 (2018) 5999–6010.
[39] Z. Jiang, Z. Li, Z. Qin, H. Sun, X. Jiao, D. Chen, LDH nanocages synthesized with MOF templates and their high performance as supercapacitors, Nanoscale 5 (2013) 11770–11775.
[40] M.J. Katz, Z.J. Brown, Y.J. Colón, P.W. Siu, K.A. Scheidt, R.Q. Snurr, J.T. Hupp, O. K. Farha, A facile synthesis of UiO-66, UiO-67 and their derivatives, Chem. Commun. (J. Chem. Soc. Sect. D) 49 (2013) 9449–9451.
[41] S.N. Kim, J. Kim, H.Y. Kim, H.Y. Cho, W.-S. Ahn, Adsorption/catalytic properties of MIL-125 and $NH_2$-MIL-125, Catal. Today 204 (2013) 85–93.
[42] X. He, C. Yang, D. Wang, S.E. Gilliland III, D.R. Chen, W.N. Wang, Facile synthesis of ZnO@ ZIF core–shell nanofibers: crystal growth and gas adsorption, CrystEngComm 19 (2017) 2445–2450.
[43] H. Lee, D. Segets, S. Süß, W. Peukert, S.C. Chen, D.Y.H. Pui, Liquid filtration of nanoparticles through track-etched membrane filters under unfavorable and different ionic strength conditions: experiments and modeling, J. Membr. Sci. 524 (2017) 682–690.
[44] S.C. Chen, D. Segets, T.Y. Ling, W. Peukert, D.Y.H. Pui, An experimental study of ultrafiltration for sub-10 nm quantum dots and sub-150 nm nanoparticles through PTFE membrane and Nuclepore filters, J. Membr. Sci. 497 (2016) 153–161.
[45] M. Tang, D. Thompson, S.C. Chen, Y. Liang, D.Y.H. Pui, Environment, Evaluation of different discharging methods on HVAC electret filter media, Build. Environ. 141 (2018) 206–214.
[46] C.Y. Tien, J.P. Chen, S. Li, Z. Li, Y.M. Zheng, A.S. Peng, F. Zhou, C.J. Tsai, S. C. Chen, Experimental and theoretical analysis of loading characteristics of different electret media with various properties toward the design of ideal depth filtration for nanoparticles and fine particles, Separ. Purif. Technol. 233 (2020), 116002.
[47] K. Vellingiri, P. Kumar, A. Deep, K.H. Kim, Metal-organic frameworks for the adsorption of gaseous toluene under ambient temperature and pressure, Chem. Eng. J. 307 (2017) 1116–1126.
[48] M. Lillo-Ródenas, D. Cazorla-Amorós, A. Linares-Solano, Behaviour of activated carbons with different pore size distributions and surface oxygen groups for benzene and toluene adsorption at low concentrations, Carbon 43 (2005) 1758–1767.
[49] J.M. Kim, J.H. Kim, C.Y. Lee, D.W. Jerng, H.S. Ahn, Toluene and acetaldehyde removal from air on to graphene-based adsorbents with microsized pores, J. Hazard Mater. 344 (2018) 458–465.
[50] J. Mohammed, N.S. Nasri, M.A.A. Zaini, U.D. Hamza, F.N. Ani, Biodegradation, Adsorption of benzene and toluene onto KOH activated coconut shell based carbon treated with $NH_3$, Int. Biodeterior. Biodegrad. 102 (2015) 245–255.
[51] B. Kim, Y.R. Lee, H.Y. Kim, W.S. Ahn, Adsorption of volatile organic compounds over MIL-125-NH2, Polyhedron 154 (2018) 343–349.
[52] S. Hu, M. Liu, K. Li, Y. Zuo, A. Zhang, C. Song, G. Zhang, X. Guo, Solvothermal synthesis of NH 2-MIL-125 (Ti) from circular plate to octahedron, CrystEngComm 16 (2014) 9645–9650.
[53] M.J. Lashaki, M. Fayaz, S. Niknaddaf, Z. Hashisho, Effect of the adsorbate kinetic diameter on the accuracy of the Dubinin–Radushkevich equation for modeling adsorption of organic vapors on activated carbon, J. Hazard Mater. 241 (2012) 154–163.
[54] C.E. Webster, R.S. Drago, M.C. Zerner, Molecular dimensions for adsorptives, J. Am. Chem. Soc. 120 (1998) 5509–5516.
[55] K. Yang, Q. Sun, F. Xue, D. Lin, Adsorption of volatile organic compounds by metal-organic frameworks MIL-101: influence of molecular size and shape, J. Hazard Mater. 195 (2011) 124–131.
[56] P.W. Seo, B.N. Bhadra, I. Ahmed, N.A. Khan, S.H. Jhung, Adsorptive removal of pharmaceuticals and personal care products from water with functionalized metal-organic frameworks: remarkable adsorbents with hydrogen-bonding abilities, Sci. Rep. 6 (2016) 34462.
[57] M. Wen, G. Li, H. Liu, J. Chen, T. An, H. Yamashita, Metal-organic framework-based nanomaterials for adsorption and photocatalytic degradation of gaseous pollutants: recent progress and challenges, Environ. Sci. Nano 6 (2019) 1006–1025.